Separation Science and Technology
Publication details, including instructions for authors and subscription information:
http://www.informaworld.com/smpp/title~content=t713708471

A Mechanistic Study of Uphill Transport of Metal Ions through Countertransport Supported Liquid Membranes

Ruey-Shin Juang[a]; Hwai-Luh Chang[a]
[a] DEPARTMENT OF CHEMICAL ENGINEERING, YUAN-ZE INSTITUTE OF TECHNOLOGY, TAOYUAN, TAIWAN, REPUBLIC OF CHINA

To cite this Article Juang, Ruey-Shin and Chang, Hwai-Luh(1996) 'A Mechanistic Study of Uphill Transport of Metal Ions through Countertransport Supported Liquid Membranes', Separation Science and Technology, 31: 3, 365 — 379
To link to this Article: DOI: 10.1080/01496399608000701
URL: http://dx.doi.org/10.1080/01496399608000701

SEPARATION SCIENCE AND TECHNOLOGY, 31(3), pp. 365–379, 1996

A Mechanistic Study of Uphill Transport of Metal Ions through Countertransport Supported Liquid Membranes

RUEY-SHIN JUANG* and HWAI-LUH CHANG
DEPARTMENT OF CHEMICAL ENGINEERING
YUAN-ZE INSTITUTE OF TECHNOLOGY
NEI-LI, TAOYUAN 32026, TAIWAN, REPUBLIC OF CHINA

ABSTRACT

The uphill transport of vanadium(IV) through a countertransport supported liquid membrane containing di(2-ethylhexyl)phosphoric acid (D2EHPA) as a mobile carrier was examined as it relates to its transport mechanism. The experiments were carried out in a stirred permeation cell with well-defined hydrodynamics. A transport model was presented that takes into account all possible resistances. The degree of uphill transport was found to depend strongly upon the transport mechanism, especially as the concentration of vanadium(IV) in the strip phase was greater than that in the feed phase. In general, the degree of uphill transport remained comparatively larger when the role of membrane diffusion was more significant.

Key Words. Uphill transport; Countertransport supported liquid membrane; D2EHPA; Vanadium(IV); Transport mechanism

INTRODUCTION

Liquid membranes containing mobile complexing carriers have been shown to be effective and attractive for the selective separation and concentration of the solute of interest from dilute solutions (1). These solutes include metal ions, weak acids and bases, hydrocarbons or biologically

* To whom correspondence should be addressed.

important compounds, and gaseous mixtures. The transport of the solute through liquid membranes, which couples the flow of two or more species, is known as coupled-transport. When these reactions produce two fluxes in opposite directions, the behavior is called countertransport. When the solute, the coupled species, and the mobile carrier engender two fluxes in the same direction, the behavior is called cotransport (1–3).

A supported liquid membrane (SLM) which uses a porous membrane support impregnated with complexing carriers to separate the feed and strip phases represents one of the feasible types of liquid membranes (1–15). The use of carrier-coupled SLM in the separation and concentration of metal species has received much attention as a possible alternative to solvent extraction because of the uphill transport or chemical pumping of a metal species against its concentration gradient (2, 3).

The uphill transport of metal species, through either a counter- or cotransport SLM, has been extensively studied since the early 1970s (4–10). For example, Cussler (4) described the countertransport of Na^+ and H^+ across a monensin/hexanol SLM. The large pumping observed experimentally can be explained by a theory based on the rapid competitive reaction of the carrier with two simultaneously diffusing solutes. Caracciolo et al. (5) demonstrated the cotransport of K^+ and Cl^- through a dibenzo-18-crown-6/tetrachloroethane bulk liquid membrane. This process can pump K^+ against its concentration gradient up to 30%. Baker et al. (6) examined the counter-transport of Cu^{2+} and H^+, using LIX 64N/kerosene, across a microporous membrane. Under favorable conditions, Cu^{2+} is concentrated 4000-fold. Babcock et al. (7) studied the cotransport of UO_2^{2+} and SO_4^{2-} through a Alamine 336-SLM and found that the final concentration factor can be greater than 2000 times the initial concentration. Matsuoka et al. (8) studied the cotransport of UO_2^{2+} and NO_3^- by entrapping tributyl phosphate in a cellulose triacetate membrane. No transport occurs when the feed phase initially contains UO_2^{2+} and the strip phase contains no UO_2^{2+}, though the concentration gradient of coupling NO_3^- exists. Moreover, Babcock et al. (9) showed the selective uphill transport of uranium from hydrometallurgical leach solutions containing iron, vanadium, and molybdenum in admixture by a tertiary amine.

In all of the above-mentioned studies, however, the uphill transport observed from SLM experiments was not analyzed theoretically (8) or was qualitatively described only by assuming that membrane diffusion is rate-controlling (4–7, 9). The assumption that only diffusion in the membrane is regarded as a possible resistance to the carrier-coupled SLM transport process is somewhat critical (11, 13, 15). This situation may be due to the lack of information on the cell hydrodynamics and the kinetic scheme of chemical reaction occurring at the aqueous–organic (mem-

brane) interface. Recently, Kim and Stroeve (10) theoretically analyzed the uphill behavior of cotransport in the parallel flat or tubular membrane separator. The effect of diffusion and reaction parameters were examined in terms of the wall Sherwood number and the dimensionless equilibrium constant, respectively. Nevertheless, the influence of the contribution of chemical reactions was not clarified.

In our earlier work (16) the countertransport of VO^{2+} across a di(2-ethylhexyl)phosphoric acid (D2EHPA) SLM was proven to be governed by mixed membrane diffusion and chemical reaction under typical SLM experimental ranges. In this paper the phenomena of uphill VO^{2+} transport is investigated experimentally and compared with the calculated results by considering all possible resistances during transport. The dependence of uphill transport on the transport mechanism is also emphasized and discussed.

TRANSPORT MODEL

Solvent Extraction Chemistry

The reaction stoichiometry for the extraction of VO^{2+} from sulfate solutions with D2EHPA in kerosene at low organic loadings can be expressed as (17)

$$VO^{2+} + (3/2)\overline{(HR)_2} \Leftrightarrow \overline{VOR_2(HR)} + 2H^+ \qquad (1)$$

where $\overline{(HR)_2}$ represents the D2EHPA dimers and the overbar refers to the organic (membrane) phase. The extraction equilibrium constant of Eq. (1), K_{ex}, is given by

$$K_{ex} = \frac{[\overline{VOR_2(HR)}][H^+]^2}{[VO^{2+}][\overline{(HR)_2}]^{3/2}} \qquad (2)$$

In the present study the organic loading was kept low enough so that the complex formulation of Eq. (1) was established. The value of K_{ex} under consideration has been obtained as 20.3 $(mol/m^3)^{1/2}$ at 298 K (17).

The kinetics of VO^{2+} extraction from sulfate media with kerosene solutions of D2EHPA has been examined using a membrane-based permeation cell (18). In this apparatus the contribution of diffusion resistance to the overall extraction process can be estimated and eliminated by correlating the rate data to interfacial concentrations of reactive species. Under the conditions studied, the intrinsic formation rate of the complex $\overline{VOR_2(HR)}$ per unit area, R, is given by (18)

$$R = k_1[VO^{2+}][H^+]^{-1/2}[\overline{(HR)_2}]^{1/2} - k_{-1}[\overline{VOR_2}][H^+][\overline{(HR)_2}]^{-1/2}, \qquad K_{ex} = k_1/k_{-1} \qquad (3)$$

where k_1 and k_{-1} are the forward and backward rate constants, respectively. They are determined to be 4.19×10^{-7} m/s and 1.96×10^{-8} $(m^5/mol \cdot s^2)^{1/2}$ at 298 K (16, 18). For simplicity, the organic complex $\overline{VOR_2(HR)}$ is written as $\overline{VOR_2}$ hereafter.

SLM Transport Model

The concentration profile of species through a D2EHPA-SLM is shown in Fig. 1. All possible steps are essentially considered in the present transport model, including 1) diffusion of VO^{2+} and H^+ across both aqueous stagnant layers of feed and strip phases, 2) diffusion of D2EHPA itself (monomer and dimer) and the complex in the membrane phase, and 3) chemical reaction of VO^{2+} and D2EHPA at both aqueous–membrane interfaces. The steady-state transport rates of these steps are as follows.

1–2. Diffusion of VO^{2+} and H^+ in the feed phase toward the membrane:

$$J_1 = k_{VO,f}([VO^{2+}]_f - [VO^{2+}]_{f,i}) \tag{4}$$

$$J_2 = k_{H,f}([H^+]_{f,i} - [H^+]_f) \tag{5}$$

3. Formation reaction of the complex at the feed–membrane interface (Eq. 3):

$$J_3 = k_1([VO^{2+}]_{f,i}[H^+]_{f,i}^{-1/2}[\overline{(HR)_2}]_{f,i}^{1/2} - K_{ex}^{-1}[\overline{VOR_2}]_{f,i}[H^+]_{f,i}[\overline{(HR)_2}]_{f,i}^{-1/2}) \tag{6}$$

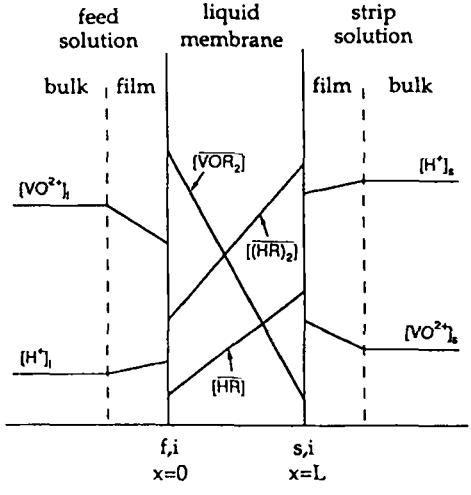

FIG. 1 Concentration profiles of the species through a D2EHPA-SLM.

4–6. Diffusion of the complex and carrier through the liquid membrane:

$$J_4 = k_{\mathrm{VOR}_2,\mathrm{m}}([\overline{\mathrm{VOR}_2}]_{\mathrm{f,i}} - [\overline{\mathrm{VOR}_2}]_{\mathrm{s,i}}) \tag{7}$$

$$J_5 = k_{(\mathrm{HR})_2,\mathrm{m}}([\overline{(\mathrm{HR})_2}]_{\mathrm{s,i}} - [\overline{(\mathrm{HR})_2}]_{\mathrm{f,i}}) \tag{8}$$

$$J_6 = k_{\mathrm{HR,m}}([\overline{\mathrm{HR}}]_{\mathrm{s,i}} - [\overline{\mathrm{HR}}]_{\mathrm{f,i}}) \tag{9}$$

7. Dissociation reaction of the complex at the membrane–strip interface:

$$\begin{aligned} J_7 = {} & k_{-1}([\overline{\mathrm{VOR}_2}]_{\mathrm{s,i}}[\mathrm{H}^+]_{\mathrm{s,i}}[\overline{(\mathrm{HR})_2}]_{\mathrm{s,i}}^{-1/2} \\ & - K_{\mathrm{ex}}[\mathrm{VO}^{2+}]_{\mathrm{s,i}}[\mathrm{H}^+]_{\mathrm{s,i}}^{-1/2}[\overline{(\mathrm{HR})_2}]_{\mathrm{s,i}}^{1/2}) \end{aligned} \tag{10}$$

8–9. Diffusion of VO^{2+} and H^+ in the strip phase outside the membrane:

$$J_8 = k_{\mathrm{VO,s}}([\mathrm{VO}^{2+}]_{\mathrm{s,i}} - [\mathrm{VO}^{2+}]_{\mathrm{s}}) \tag{11}$$

$$J_9 = k_{\mathrm{H,s}}([\mathrm{H}^+]_{\mathrm{s}} - [\mathrm{H}^+]_{\mathrm{s,i}}) \tag{12}$$

These flux equations are basically similar to those presented earlier in the countertransport of Zn^{2+} through a dithizone-SLM (13) and in the kinetic studies of Cu^{2+} extraction with LIX 65N using a rotating diffusion cell (19). In comparison with the present model, however, the nature of carrier (dimer or monomer) and the rate equations (Eqs. 6–10) are different from those in the former paper (13); moreover, the counterdiffusion of carriers (Eqs. 8 and 9) was not considered in the earlier work (19).

The solubility of D2EHPA carriers in acidic aqueous solutions is reported to be negligibly small (14–18, 20), so the total amount of D2EHPA in the membrane phase is kept constant.

$$[\overline{\mathrm{HR}}]_0 = \frac{1}{L}\int_0^L ([\overline{\mathrm{HR}}] + 2[\overline{(\mathrm{HR})_2}] + 3[\overline{\mathrm{VOR}_2}])\, dx \tag{13}$$

Assuming that the concentration profile of species in the membrane phase is linear, we have

$$\begin{aligned} [\overline{\mathrm{HR}}]_0 = {} & (1/2)([\overline{\mathrm{HR}}]_{\mathrm{f,i}} + [\overline{\mathrm{HR}}]_{\mathrm{s,i}}) + K_2([\overline{\mathrm{HR}}]_{\mathrm{f,i}}^2 + [\overline{\mathrm{HR}}]_{\mathrm{s,i}}^2) \\ & + (3/2)([\overline{\mathrm{VOR}_2}]_{\mathrm{f,i}} + [\overline{\mathrm{VOR}_2}]_{\mathrm{s,i}}) \end{aligned} \tag{14}$$

where K_2 is the dimerization constant of D2EHPA in the organic phase, namely,

$$2\overline{\mathrm{HR}} \Leftrightarrow \overline{(\mathrm{HR})_2}, \qquad K_2 = [\overline{(\mathrm{HR})_2}]/[\overline{\mathrm{HR}}]^2 \tag{15}$$

The value of K_2 in kerosene is adopted to be 12 m^3/mol at 298 K (20). Because counterdiffusion of D2EHPA itself and its metal complex occurs in the membrane phase, the continuity of the total flux of D2EHPA is

expressed by

$$J_4 = \frac{2J_5}{3} + \frac{J_6}{3} \tag{16}$$

At steady state, the following equality holds:

$$J_1 = \frac{J_2}{2} = J_3 = J_4 = J_7 = J_8 = \frac{J_9}{2} = J_{VO} \tag{17}$$

Provided that the mass transfer coefficients in Eqs. (4)–(12) are available, it is possible to calculate the steady-state transport rate, J_{VO}, by solving the system of Eqs. (4)–(12) with the additional conditions of Eqs. (14)–(17) using a trial-and-error method.

EXPERIMENTAL

Apparatus, Membrane, and Solutions

The permeation cell used in this study is illustrated in Fig. 2. Two chambers were stirred at the same speed (300 rpm) but in the opposite direc-

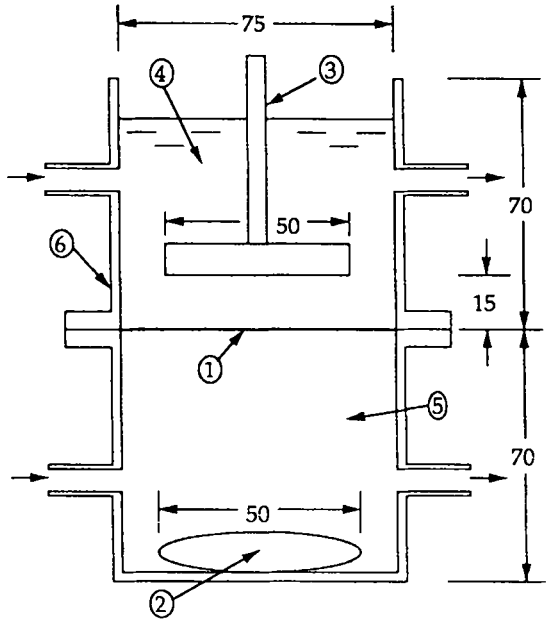

FIG. 2 The stirred permeation cell used for measuring the transport rates. (1) supported liquid membrane, (2) magnetic stirrer, (3) PTFE impeller, (4) strip phase, (5) feed phase, and (6) Pyrex glass cell. Dimensions given in millimeters.

tions. The entire cell was immersed in a thermostat controlled at 298 K. The microporous membrane used was a hydrophobic PVDF disk filter (Durapore GVHP, Millipore Co.). It had a nominal thickness of 125 μm, an average pore size of 0.22 μm, and a porosity of 75%.

The source and pretreatment of D2EHPA, kerosene, and all other inorganic chemicals were the same as those described previously (14). The membrane solution was prepared by diluting D2EHPA with kerosene and presaturating with the metal-free aqueous phase. The pores in the membrane support were filled with D2EHPA under vacuum as reported elsewhere (12, 14), and the resulting liquid membranes were immersed in the membrane phase before use.

The experimental conditions investigated in this work are listed in Table 1. The feed and strip phases were prepared by dissolving $VOSO_4$ in distilled water, to which Na_2SO_4 and H_2SO_4 were added to maintain a 500 mol/m^3 total sulfate concentration. The aqueous pH was adjusted by changing the fraction of the combination of Na_2SO_4 and H_2SO_4. All aqueous phases were presaturated with kerosene.

Experimental Procedure

In the beginning of each run, the membrane impregnated with D2EHPA was first clamped and the apparatus was assembled. Feed and strip phases were then introduced into the upper and lower chambers, respectively, and the mixing was started. When steady state was reached (about 30 minutes), a sample (5 cm^3) was taken from the feed phase at preset intervals, and more original solution was immediately added to maintain the volume unchanged. The aqueous pH values were measured with a pH meter (Radiometer Model PHM82). The concentration of VO^{2+} in the

TABLE 1
The Experimental Condition Sets Investigated in This Work[a]

Set	$[VO^{2+}]$	pH_f	$\overline{[(HR)_2]}_0$	β	J_{VO}	Δ_a	Δ_c	Δ_m
A	11.8	1.30	502	17.4	1.7×10^{-5}	0.05	0.85	0.10
B				4.7	1.4×10^{-5}	0.04	0.88	0.08
C	38.5	2.01	250	17.4	4.0×10^{-5}	0.02	0.73	0.25
D				4.7	2.2×10^{-5}	0.02	0.83	0.15
E	10.5	3.66	90	2440	2.6×10^{-5}	0.08	0.42	0.50
F				1000	2.3×10^{-5}	0.07	0.48	0.45
G				17.4	3.0×10^{-6}	0.01	0.90	0.09
H				10	2.4×10^{-6}	0.01	0.93	0.06

[a] The measured values of J_{VO} and the calculated values of Δ_a, Δ_c, and Δ_m are shown at $\alpha = 0$. The unit of each symbol is given in the Nomenclature Section.

sample was analyzed with an UV-visible spectrophotometer (Hitachi Model U-3410) at a wavelength of 445 nm (17), and corrections due to volume replacement were made. The steady-state transport rate, J_{VO}, was obtained according to

$$J_{VO} = -(V_f/S)\,(d[VO^{2+}]_f/dt) \tag{18}$$

RESULTS AND DISCUSSION

Under the conditions investigated, the mass transfer coefficients pertinent to the present permeation cell shown in Eqs. (4)–(12) were measured or correlated earlier (16, 18). They, together with the equilibrium and kinetic parameters of solvent extraction, are compiled in Table 2. Since VO^{2+} is expected to be "chemically pumped" through a D2EHPA-SLM against its concentration gradient by allowing the counter-flow of a coupled H^+, the following two parameters are defined and will be used in the discussion of uphill transport in this work.

$$\alpha = [VO^{2+}]_s/[VO^{2+}]_f \quad \text{and} \quad \beta = [H^+]_s/[H^+]_f \tag{19}$$

The degree of uphill transport, Φ, for a fixed value of β is defined as

$$\Phi = J_{VO}|_{\alpha=\alpha}/J_{VO}|_{\alpha=0} \tag{20}$$

TABLE 2
Values of Parameters Used for the Calculation of Transport Rates in This Work

Parameter	VO^{2+}/D2EHPA-SLM system	Reference
Dimerization constant:		
K_2	12 m^3/mol	20
Extraction equilibrium constant:		
K_{ex}	20.3 $(mol/m^3)^{1/2}$	18
Reaction rate constant:		
k_1	4.19×10^{-7} m/s	18
k_{-1}	1.96×10^{-8} $(m^5/mol \cdot s^2)^{1/2}$	18
Mass transfer coefficient:		
$k_{VO,f}$, $k_{VO,s}$	3.80×10^{-5} m/s	16
$k_{H,f}$, $k_{H,s}$	1.40×10^{-4} m/s	16
$k_{VOR_2,m}$	8.52×10^{-7} m/s	16
$k_{(HR)_2,m}$	1.16×10^{-6} m/s	16
$k_{HR,m}$	1.80×10^{-6} m/s	16

Figures 3–5 show the degree of uphill transport under various condition sets. The solid curves in these figures were calculated by the present transport model. Close agreement between the measured and calculated rates is observed (average standard error, 5%). In the majority of cases studied, an increase in the value of α, the degree of uphill transport, either slightly decreases or remains nearly constant when $\alpha < 1$, but decreases sharply when $\alpha > 1$.

The transport resistances due to aqueous layer diffusion, interfacial chemical reaction, and membrane diffusion were measured to clarify the dependence of degree of uphill transport on the transport mechanism. For $\alpha = 0$, the rate equations under these extreme conditions are given as follows.

1. Aqueous layer diffusion control, $J_{VO,a}$:

$$J_{VO,a} = k_{VO,f}[VO^{2+}]_f \tag{21}$$

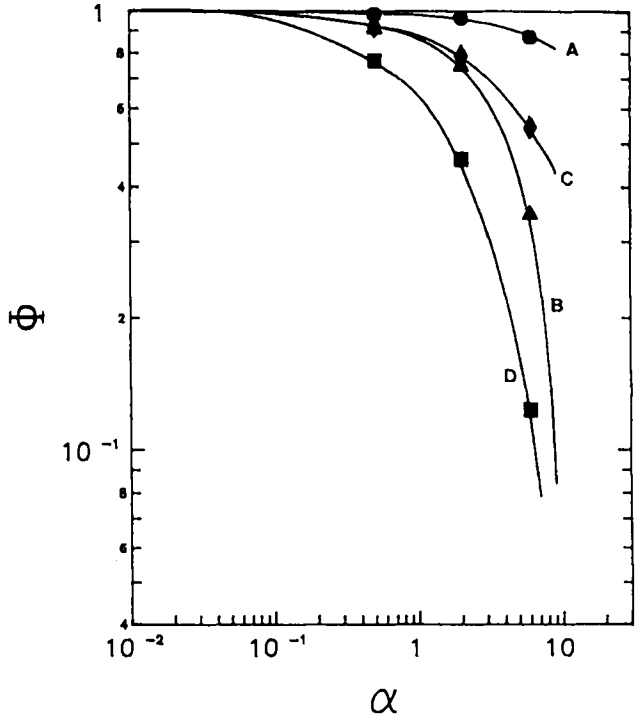

FIG. 3 Dependence of the degree of uphill transport on the value of α for condition sets A–D. The solid curves are calculated by the transport model.

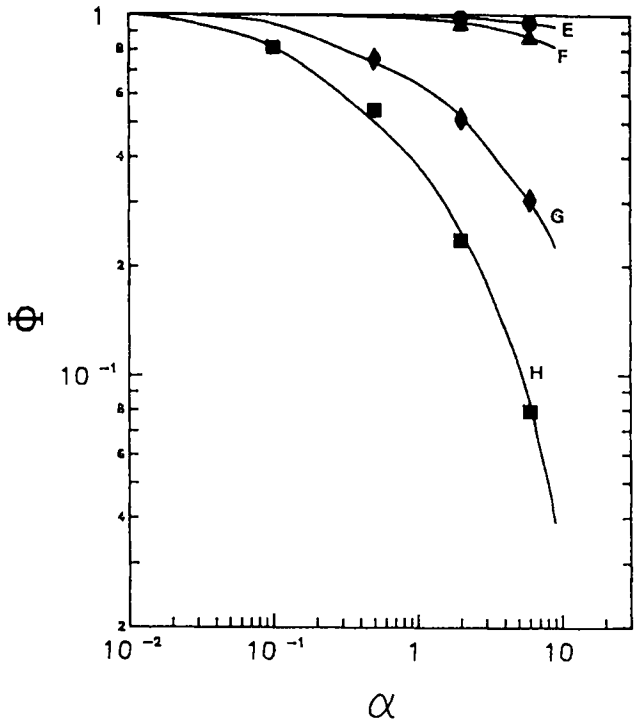

FIG. 4 Dependence of the degree of uphill transport on the value of α for condition sets E–H. The solid curves are calculated by the transport model.

2. Interfacial chemical reaction control, $J_{VO,c}$:

$$J_{VO,c} = k_1([VO^{2+}]_f[H^+]_f^{-1/2}[\overline{(HR)_2}]_{f,i}^{1/2} - K_{ex}^{-1}[\overline{VOR_2}]_{f,i}[H^+]_f[\overline{(HR)_2}]_{f,i}^{-1/2}) \quad (22)$$

3. Membrane diffusion control, $J_{VO,m}$:

$$J_{VO,m} = k_{VOR_{2,m}}[\overline{VOR_2}]_{f,i} \quad (23)$$

Conceptually, the fractional resistance of the respective step to overall transport process, Δ_a, Δ_c, and Δ_m, can be calculated according to Eqs. (24)–(26).

$$\Delta_a = \frac{(1/J_{VO,a})}{(1/J_{VO,a}) + (1/J_{VO,c}) + (1/J_{VO,m})} \quad (24)$$

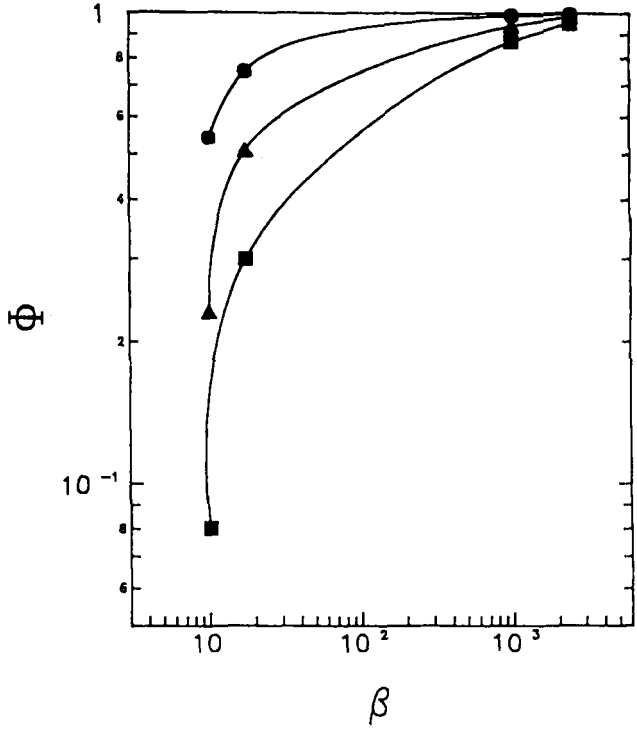

FIG. 5 Dependence of the degree of uphill transport on the value of β for condition sets E–H. α = 0.5 (●), 2 (▲), and 6 (■). The solid curves are calculated by the transport model.

$$\Delta_c = \frac{(1/J_{VO,c})}{(1/J_{VO,a}) + (1/J_{VO,c}) + (1/J_{VO,m})} \tag{25}$$

$$\Delta_m = \frac{(1/J_{VO,m})}{(1/J_{VO,a}) + (1/J_{VO,c}) + (1/J_{VO,m})} \tag{26}$$

In other words, the rate-determining steps during transport can be identified quantitatively by comparing the values of Δ_a, Δ_c, and Δ_m. As shown in the last three columns of Table 1, the present transport process is mainly controlled by combined interfacial chemical reaction and membrane diffusion for the described conditions. Furthermore, the value of Δ_c is found to be larger for lower β, whereas the value of Δ_m is larger for higher β. In fact, the above results are obtained only for $\alpha = 0$. It is highly desired to calculate the values of Δ_a, Δ_c, and Δ_m when the value of α is varied.

They are listed in Table 3. It is evident that the value of Δ_c increases with the value of α, but values of both Δ_a and Δ_m decrease.

As clearly seen in Figs. 3–5, under the same base conditions (i.e., sets A–B, C–D, and E–G) the degree of uphill transport remains relatively larger for either higher β or lower α; both correspond to situations where the role of membrane diffusion becomes more important. This may be explained by the fact that the uphill transport of solute is acting against its "concentration gradient" between the membrane by coupling the flow of the other species. It should be noted that the separation behavior of Co^{2+} and Ni^{2+} across an SLM containing 2-ethylhexyl phosphonic acid mono-2-ethylhexyl ester as mobile carriers (12) and of Zn^{2+} and Cu^{2+} through a D2EHPA-SLM (14) may be interrelated with the present findings. Higher selectivity is obtained when diffusional resistance in the membrane phase is more dominant.

Several related results have been reported previously in the coupled-transport SLM processes. For example, Baker et al. (6) studied the countertransport of Cu^{2+} and H^+ across an LIX64N-SLM. The concentration factor (equivalent to the degree of uphill transport) is highly sensitive to the strip pH, and the flux of Cu^{2+} increases as the strip pH decreases. Kim and Stroeve (10) analyzed numerically the uphill behavior of cotransport in the parallel plate or tubular membrane separator. The degree of uphill transport increased with the maximum cotransport factor (equivalent to the concentration difference of the coupled species). Also, by increasing the dimensionless equilibrium constant, the degree of uphill transport decreases. This is attributed to the fact that the chemical reaction is essentially saturated within the membrane and the cotransport flux is small when the dimensionless equilibrium constant is large. Furthermore, the

TABLE 3
The Calculated Values of Δ_a, Δ_c, and Δ_m, under Different Conditions

No.	$[VO^{2+}]_f$	pH_f	$[\overline{(HR)_2}]_0$	α	β	Δ_a	Δ_c	Δ_m
1	41	1.91	250	0.12	6.9	0.02	0.78	0.20
2				0.37		0.02	0.78	0.20
3				1.37		0.01	0.83	0.16
4				2.93		0.01	0.87	0.12
5				12.2		Nil	0.97	0.03
6	41	1.91	502	0.12	6.9	0.03	0.82	0.15
7				0.37		0.03	0.82	0.15
8				1.37		0.02	0.86	0.12
9				2.93		0.01	0.90	0.09
10				12.2		Nil	0.98	0.02

degree of uphill transport is increased with the wall Sherwood number, defined as the ratio of mass transfer resistance in the aqueous film to that in the membrane.

An attempt was also made in this study to extend the above observation that the degree of uphill transport is larger when the role of membrane diffusion is more dominant to different base conditions, such as the condition sets A, C, and G. Figure 6 shows the results obtained for a fixed β value of 17.4. Unfortunately, such a dependency does not exist, not even inversely, because the value of Δ_m for the upper curve (A) is not necessarily larger than that for the lower curve (C), as clearly shown in Fig. 6. However, it is surprisingly observed that the smaller the value of Δ_a, the smaller the degree of uphill transport, although Δ_a is comparatively small in the present transport process. More research efforts must apparently be made to justify such observations.

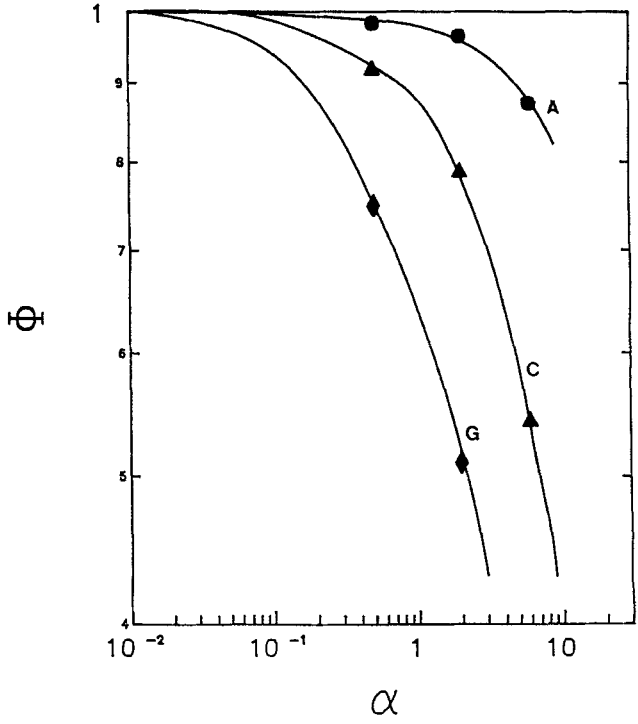

FIG. 6 Dependence of the degree of uphill transport on the value of α for condition sets A, C, and G. The solid curves are calculated by the transport model.

CONCLUSIONS

The degree of uphill transport of VO^{2+} from 500 mol/m^3 (Na,H,VO)SO_4 feed solutions through a D2EHPA-SLM has been quantitatively related to its transport mechanism. Under the conditions examined, the transport process is controlled by combined interfacial chemical reaction and membrane diffusion. In addition, the transport rates calculated from the present model are in good agreement with the measured ones (average standard deviation, 5%). For the same base conditions, the degree of uphill transport remains relatively larger whether for either higher β or lower α, both of which exactly correspond to situations in which the role of membrane diffusion becomes more important.

ACKNOWLEDGMENT

This work was supported by the ROC National Science Council under Grant NSC83-0402-E-155-014, which is greatly appreciated.

NOMENCLATURE

D2EHPA	di(2-ethylhexyl)phosphoric acid
HR	D2EHPA monomer
$(HR)_2$	D2EHPA dimer
J	transport rate (mol/m^2·s)
k	mass transfer coefficient (m/s)
k_1	forward reaction rate constant defined in Eq. (3) (m/s)
k_{-1}	backward reaction rate constant defined in Eq. (3) (m^5/mol·s^2)$^{1/2}$
K_2	dimerization constant of D2EHPA in the organic phase (m^3/mol)
K_{ex}	extraction equilibrium constant defined in Eq. (2) (mol/m^3)$^{1/2}$
R	formation reaction rate of VO^{2+} and D2EHPA per unit area (mol/m^2·s)
S	membrane cross-section area (m^2)
t	time (s)
V	volume (m^3)
[ ]	molar concentration of species in the brackets (mol/m^3)

Greek Letters

α, β	parameters defined in Eq. (19)

Δ_a, Δ_c, Δ_m	fractional resistances of aqueous layer diffusion, interfacial chemical reaction, and membrane diffusion to overall transport process, respectively
Φ	degree of uphill transport defined in Eq. (20)

Subscripts

f, m, s	feed, membrane, and strip phases, respectively
i	aqueous–membrane interface
0	initial

Superscript

$\overline{\text{(overbar)}}$	species in the membrane or organic phase

REFERENCES

1. R. D. Noble and J. D. Way, in *Liquid Membranes. Theory and Applications* (R. D. Noble and J. D. Way, Eds.), American Chemical Society, Washington, D.C., 1987, pp. 1–26.
2. P. R. Danesi, *Sep. Sci. Technol.*, *19*(11&12), 857 (1985).
3. G. Schulz, *Desalination*, *68*, 191 (1988).
4. E. L. Cussler, *AIChE J.*, *17*(6), 1300 (1971).
5. F. Caracciolo, E. L. Cussler, and D. F. Evans, *Ibid.*, *21*(1), 160 (1975).
6. R. W. Baker, M. E. Tuttle, D. J. Kelly, and H. K. Lonsdale, *J. Membr. Sci.*, *2*, 213 (1977).
7. W. C. Babcock, R. W. Baker, E. D. LaChapelle, and K. L. Smith, *Ibid.*, *7*, 71 (1980).
8. H. Matsuoka, M. Aizawa, and S. Suzuki, *Ibid.*, *7*, 11 (1980).
9. W. C. Babcock, D. T. Friesen, and E. D. LaChapelle, *Ibid.*, *26*, 303 (1986).
10. J. I. Kim and P. Stroeve, *Ibid.*, *49*, 37 (1990).
11. W. C. Babcock, R. W. Baker, E. D. LaChapelle, and K. L. Smith, *Ibid.*, *7*, 89 (1980).
12. H. Matsuyama, Y. Katayama, A. Kojima, I. Washijima, Y. Miyake, and M. Teramoto, *J. Chem. Eng. Jpn.*, *20*(3), 213 (1987).
13. P. Plucinski and W. Nitsch, *J. Membr. Sci.*, *39*, 43 (1988).
14. R. S. Juang, *Ind. Eng. Chem. Res.*, *32*(5), 911 (1993).
15. J. Marchese, M. E. Campderros, and A. Acosta, *J. Chem. Tech. Biotechnol.*, *57*(1), 37 (1993).
16. R. S. Juang and R. H. Lo, *Ind. Eng. Chem. Res.*, *33*(4), 1011 (1994).
17. R. S. Juang and R. H. Lo, *J. Chem. Eng. Jpn.*, *26*(2), 219 (1993).
18. R. S. Juang and R. H. Lo, *Ind. Eng. Chem. Res.*, *33*(4), 1001 (1994).
19. M. Jin, F. C. Michel Jr., and R. D. Noble, *Ibid.*, *28*(2), 193 (1989).
20. R. S. Juang and J. Y. Su, *Ibid.*, *31*(10), 2395 (1992).

Received by editor July 18, 1994
First revision received April 12, 1995
Second revision received July 19, 1995